Supplemental Figures and Tables

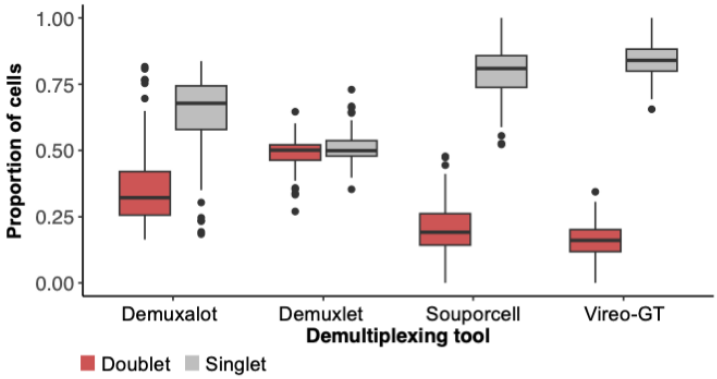

Figure S1. Proportion of doublets and singlets classified correctly by the indicated tool amongst cells correctly classified by only one tool. Genetic demultiplexing tools using prior genotype information were evaluated on 96 *in silico* pools with known ground-truth sample labels ranging in size from 4 to 80 multiplexed induced pluripotent stem cell (iPSC) lines from genetically distinct individuals, averaging 17,396 cells per pool and a 15% doublet rate.

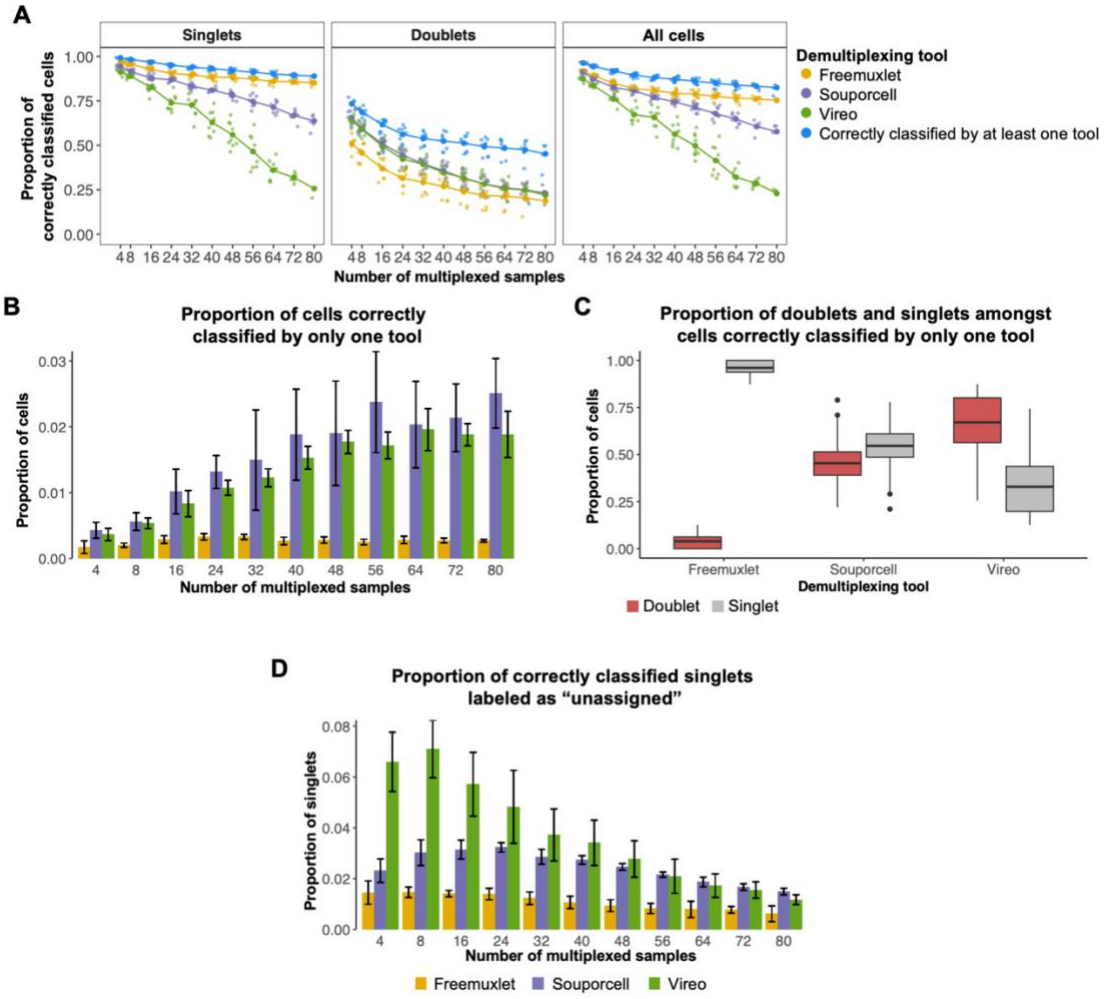

Figure S2. Evaluation of existing individual genetic demultiplexing tools when demultiplexing without prior genotype information. Evaluation of genetic demultiplexing tools with prior genotype information on 96 *in silico* pools with known ground-truth sample labels ranging in size from 4 to 80 multiplexed induced pluripotent stem cell (iPSC) lines from genetically distinct individuals, averaging 17,396 cells per pool and a 15% doublet rate. **A)** Line graphs showing the proportion of correctly classified singlets, doublets, and all cells by each individual genetic demultiplexing tool across varying numbers of multiplexed iPSC lines in a single pool (sample number). The large dots show the mean proportion of correct classifications by an individual tool across replicates at a given sample size (n = 9 per pool size). The blue points show the proportion of cells that were correctly classified by at least one individual genetic demultiplexing tool: Freemuxlet, Souporcell, or Vireo. **B)** Bar chart showing the mean proportion of total cells from an individual pool correctly classified by only one genetic demultiplexing tool. Error bars represent one standard deviation from the mean. (n = 9 per pool size) **C)** Boxplots showing the proportion of doublets and singlets classified correctly by the indicated tool amongst cells correctly classified by only one tool (n = 96 pools). **D)** Bar chart showing the proportion of correctly classified singlet cells labelled as "unassigned" (ambiguous singlet assignments) due to assignment probabilities below the recommended threshold of the respective genetic demultiplexing tool. Error bars represent one standard deviation from the mean. (n = 9 per pool size).

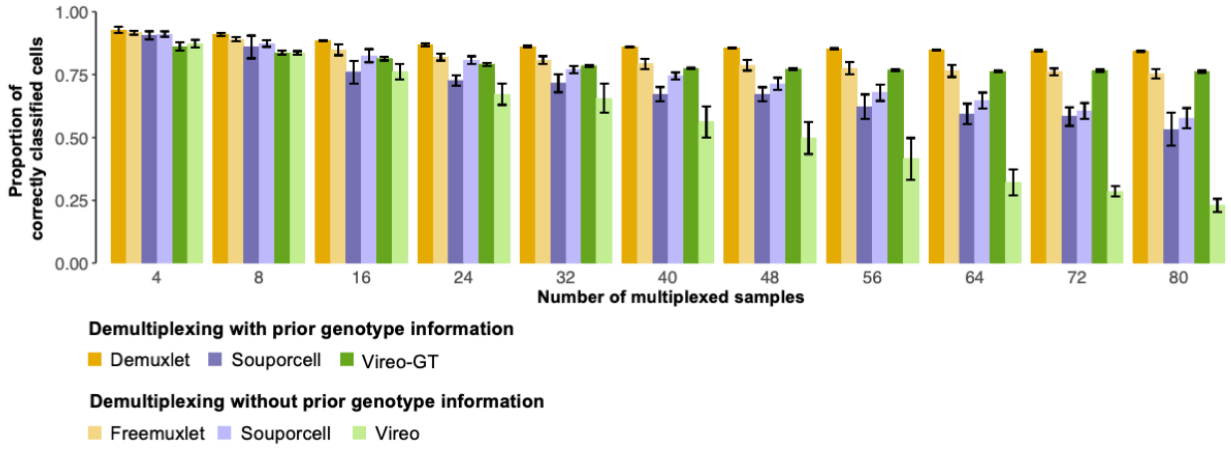

Figure S3. Comparison of genetic demultiplexing performance when demultiplexing with and without prior genotype information. Genetic demultiplexing tools were evaluated 96 *in silico* pools with known ground-truth sample labels ranging in size from 4 to 80 multiplexed induced pluripotent stem cell (iPSC) lines from genetically distinct individuals, averaging 17,396 cells per pool and a 15% doublet rate. Error bars represent one standard deviation from the mean.

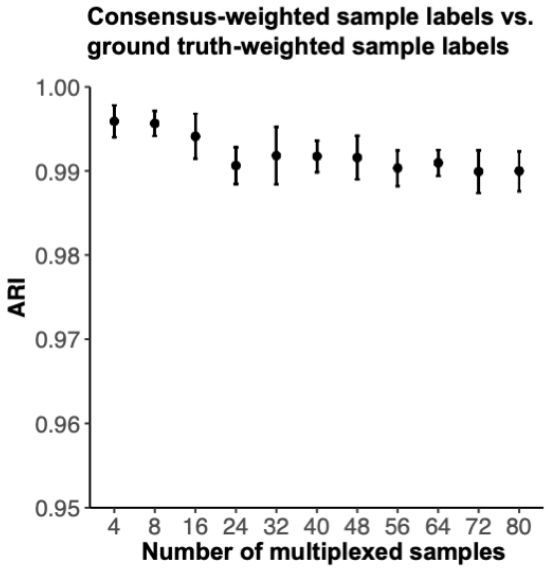

Figure S4. Validating the accuracy-weighted probabilistic ensemble component of the Ensemblex framework on *in silico* pools with known ground-truth sample labels. The accuracy-weighted probabilistic ensemble component (Step 1) of the Ensemblex framework weights the assignment probabilities from the constituent genetic demultiplexing tools by their estimated balanced accuracy for the dataset and the weighted probabilities are used to determine the most probable sample labels for each cell. The estimated balanced accuracy of an individual tool (e.g., Demuxalot) is computed on cells with a consensus sample label across the three remaining tools (e.g., Demuxlet, Souporcell, and Vireo), which Ensemblex uses as a proxy for ground-truth sample labels. To validate our approach of using the balanced accuracy derived from consensus cells for weighting each tool's assignment probabilities, we leveraged 96 *in silico* pools with known ground-truth sample labels ranging in size from 4 to 80 multiplexed induced pluripotent stem cell (iPSC) lines from genetically distinct individuals, averaging 17,396 cells per pool and a 15% doublet rate. The figure shows the mean Adjusted Rand Index (ARI) between consensus-weighted sample labels and ground-truth weighted sample labels across replicates at a given sample size. Error bars represent one standard deviation from the mean.

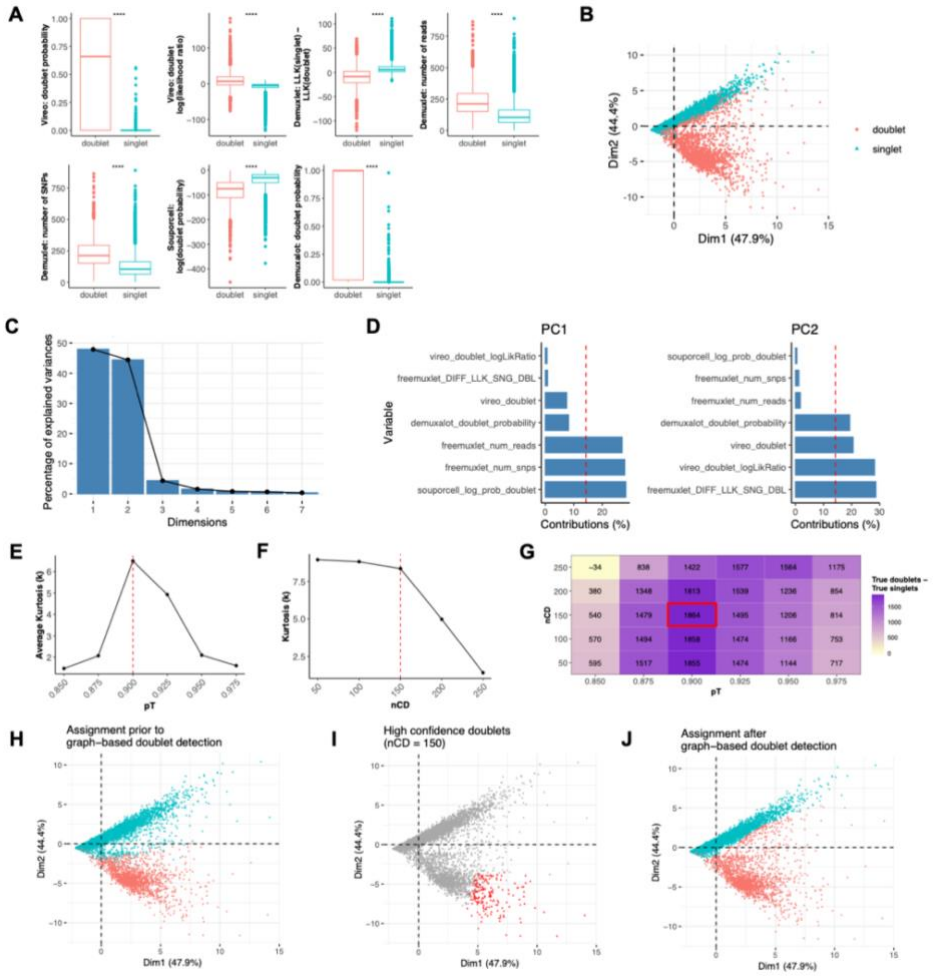

Figure S5. Demonstration of the graph-based doublet detection component of the Ensemblex framework on an *in silico* pool with known ground-truth sample labels. For this demonstration of the graph-based doublet detection component of the Ensemblex framework, we leveraged a computationally multiplexed pool comprising 24 induced pluripotent stem cell (iPSC) lines from genetically distinct individuals, 17,384 pooled cells, and a 15% doublet rate. **A)** Box plot showing the distribution of the doublet-related features across true singlets and true doublets. Wilcoxon rank-sum tests were used to compare the distribution of features across true singlets and doublets. **B)** Principal component analysis (PCA) using the doublet-related features showing true singlets and true doublets across the first two principal components (PCs). **C)** Scree plot showing the percentage of variance explained by the first seven PCs. **D)** Bar plots showing the percent contribution of each doublet-related variable to the first two PCs. **E)** Dot plot showing the average Pearson's measure of kurtosis (K) of the nearest neighbour frequency (fNN) density plots across percentile threshold (pT) values tested in the graph-based doublet detection parameter sweep. **F)** Dot plot showing K of the fNN density plots across varying numbers of confident doublet (nCD) tested in the parameter sweep for the optimal pT value (0.900). **G)** Heatmap showing the number of true doublets — the number of true singlets classified as doublets by the graph-based doublet detection component of the Ensemblex framework across various combinations of nCD and pT values tested in the parameter sweep. The red box shows the optimal nCD and pT values identified by the parameter sweep. **H)** PCA showing singlet and doublet classifications by Ensemblex after Step 1 (prior to graph-based doublet detection). **I)** PCA showing confident doublets identified by the graph-based doublet detection component

of the Ensemblex framework. The optimal nCD are shown. **J)** PCA showing singlet and doublet classifications by Ensemblex after performing graph-based doublet detection. **** P-value < 0.0001.

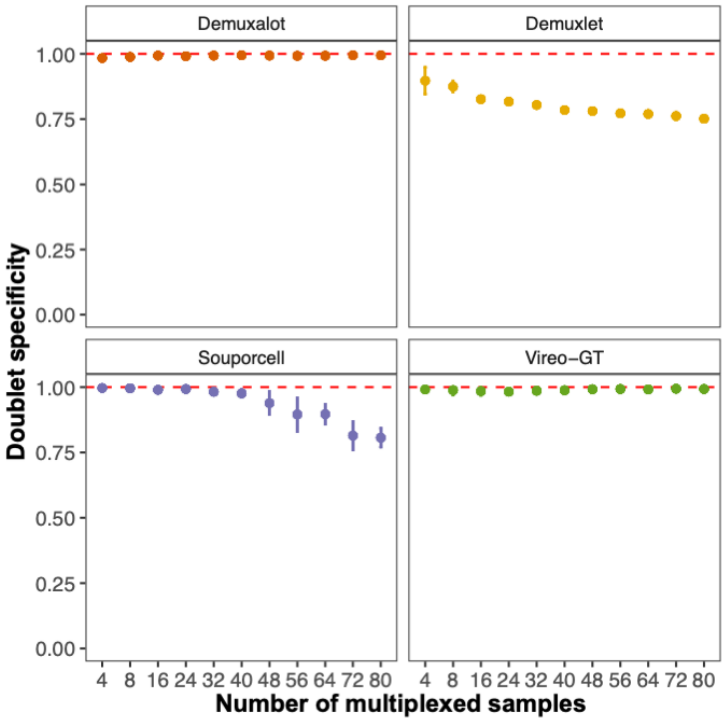

Figure S6. Validating the ensemble-independent doublet detection component of the Ensemblex framework on *in silico* pools with known ground-truth sample labels. The ensemble-independent doublet detection component of the Ensemblex framework retains the doublet labels from constituent demultiplexing tools that showed high doublet detection specificity on computationally multiplexed pools with known ground-truth sample labels. Namely, Ensemblex retains the doublet predictions made by Demuxalot and Vireo, by default. The doublet detection specificity of the individual tools was computed 96 *in silico* pools with known ground-truth sample labels ranging in size from 4 to 80 multiplexed induced pluripotent stem cell (iPSC) lines from genetically distinct individuals, averaging 17,396 cells per pool and a 15% doublet rate. The figure shows the mean doublet detection specificity of each constituent tool across replicates at a given sample size. Error bars represent one standard deviation from the mean.

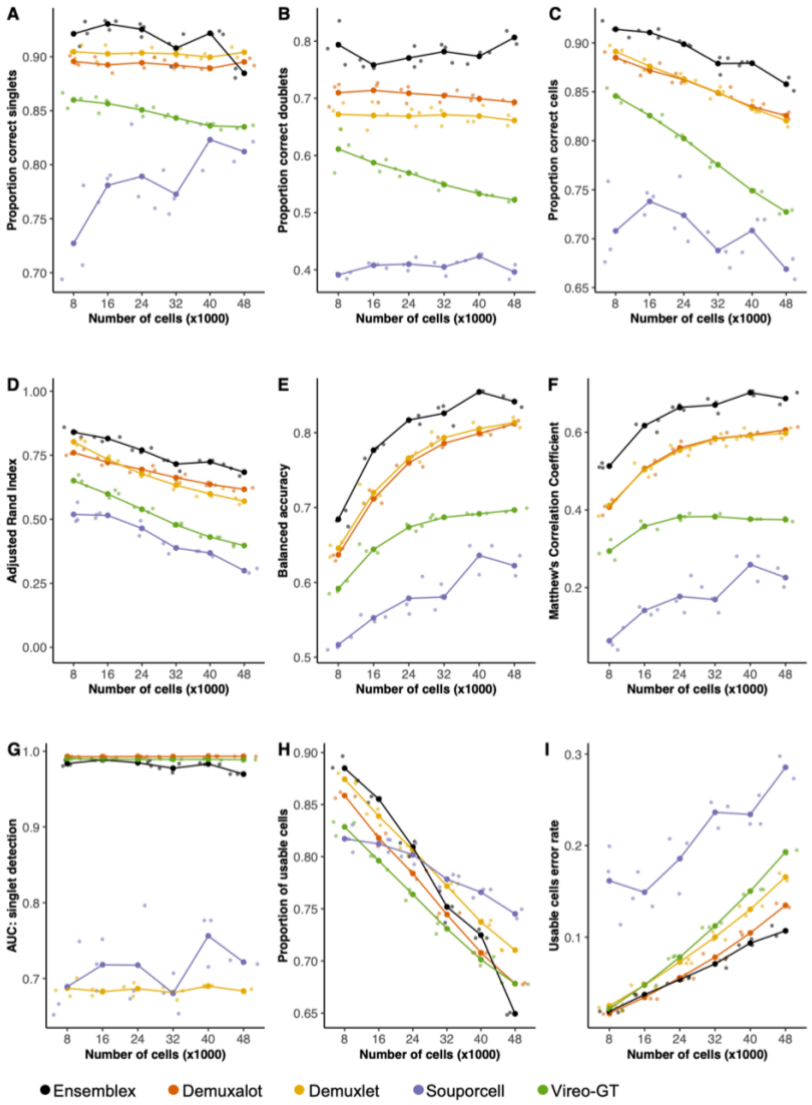

Figure S7. Genetic demultiplexing performance with prior genotype information on *in silico* pools with varying numbers of pooled cells. Genetic demultiplexing tools were evaluated on 18 *in silico* pools with known ground-truth sample labels ranging in size from 8,000 to 48,000 pooled cells with 24 multiplexed induced pluripotent stem cell (iPSC) lines from genetically distinct individuals and a doublet rate of 6% per 8,000 cells. A singlet was considered correctly classified if the assigned sample label matched the ground-truth sample label and the assignment probability exceeded the recommended threshold for the respective tool; a doublet was considered correctly classified if the assigned sample label matched the ground-truth sample label, regardless of the assignment probability. **A-I)** Line graphs showing the performance of Ensemblex and the individual genetic demultiplexing tools across evaluation metrics. The large dots show the mean value for each tool across replicates at a given pool size (n = 3 per pool size). **A)** Proportion of correctly classified singlets. **B)** Proportion of correctly classified doublets. **C)** Proportion of correctly classified cells. **D)** Adjusted Rand Index between each tool's sample labels and the ground- truth sample labels. **E)** Balanced accuracy of each tool. **F)** Matthew's Correlation Coefficient of each tool. **G)** Area under the receiver operating characteristic curve (AUC) of the singlet assignment probability for each tool. **H)** Proportion of usable cells returned by each tool. Usable cells were defined as singlets with an assignment probability exceeding the recommended threshold of the respective tool. **I)** Error rate amongst the usable cells returned by each tool; erroneous classifications comprised of true doublets labeled as singlets or true singlets assigned to the wrong sample.

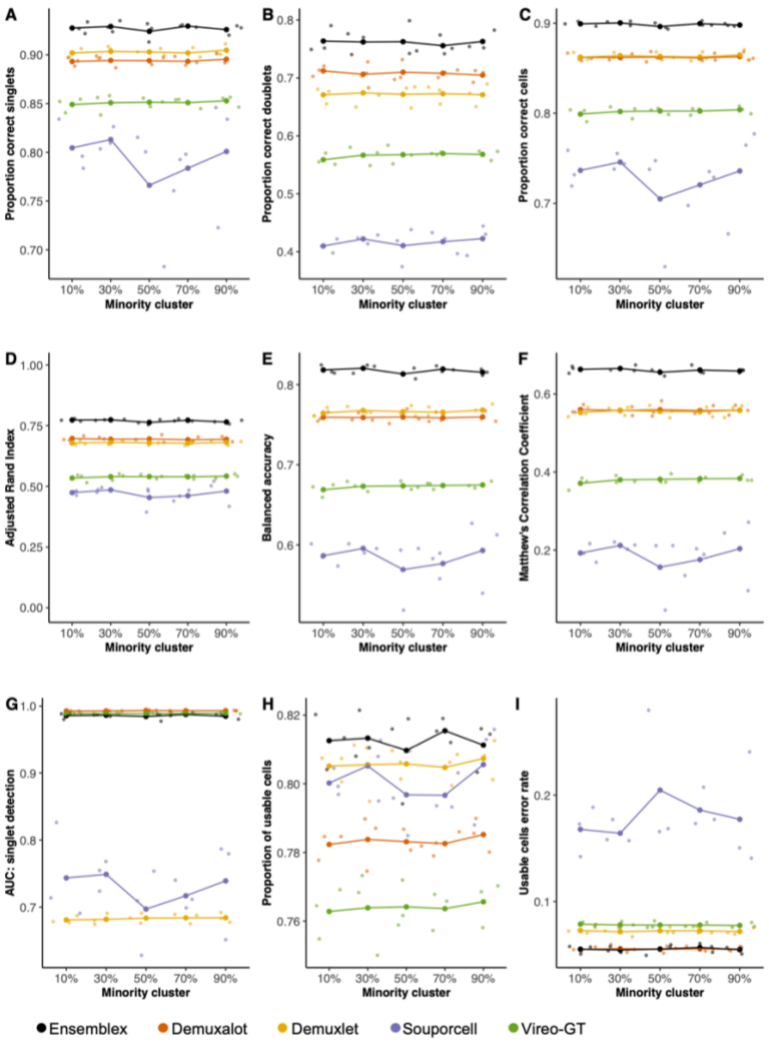

Figure S8. Genetic demultiplexing performance with prior genotype information on *in silico* pools with an underrepresented cell line. Genetic demultiplexing tools were evaluated on 15 *in silico* pools with known ground-truth sample labels, comprising 24 multiplexed induced pluripotent stem cell (iPSC) lines from genetically distinct individuals and a 15% doublet rate. For each pool, 23 iPSC lines contained 1,000 cells, while one randomly selected line showed various degrees of underrepresentation, namely 100 cells (10%), 300 cells (30%), 500 cells (50%), 700 cells (70%), or 900 cells (90%). A singlet was considered correctly classified if the assigned sample label matched the ground-truth sample label and the assignment probability exceeded the recommended threshold for the respective tool; a doublet was considered correctly classified if the assigned sample label matched the ground-truth sample label, regardless of the assignment probability. **A-I)** Line graphs showing the performance of Ensemblex and the individual genetic demultiplexing tools across evaluation metrics. The large dots show the mean value for each tool across replicates at a given degree of underrepresentation (n = 3 degree of underrepresentation). **A)** Proportion of correctly classified singlets. **B)** Proportion of correctly classified doublets. **C)** Proportion of correctly classified cells. **D)** Adjusted Rand Index between each tool's sample labels and the ground-truth sample labels. **E)** Balanced accuracy of each tool. **F)** Matthew's Correlation Coefficient of each tool. **G)** Area under the receiver operating characteristic curve (AUC) of the singlet assignment probability for each tool. **H)** Proportion of usable cells returned by each tool. Usable cells were defined as singlets with an assignment probability exceeding the recommended threshold of the respective tool. **I)** Error rate amongst the usable cells returned by each tool; erroneous classifications comprised of true doublets labeled as singlets or true singlets assigned to the wrong sample.

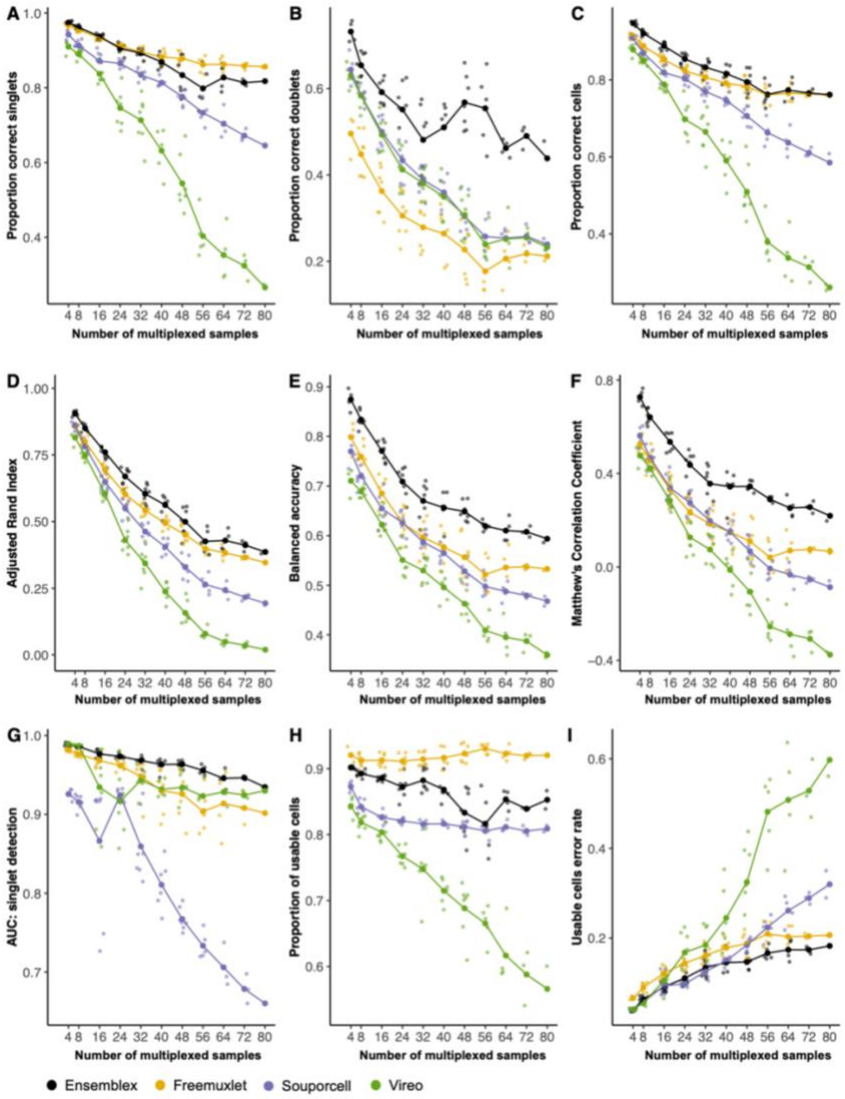

Figure S9. Genetic demultiplexing performance without prior genotype information on *in silico* pools with varying numbers of multiplexed samples. The genetic demultiplexing tools without prior genotype information were evaluated on 96 *in silico* pools with known ground-truth sample labels ranging in size from 4 to 80 multiplexed induced pluripotent stem cell (iPSC) lines from genetically distinct individuals, averaging 17,396 cells per pool and a 15% doublet rate. A singlet was considered correctly classified if the assigned sample label matched the ground-truth sample label and the assignment probability exceeded the recommended threshold for the respective tool; a doublet was considered correctly classified if the assigned sample label matched the ground-truth sample label, regardless of the assignment probability. **A-I)** Line graphs showing the performance of Ensemblex and the individual genetic demultiplexing tools across evaluation metrics. The large dots show the mean value for each tool across replicates at a given sample size (n = 9 per pool size). **A)** Proportion of correctly classified singlets. **B)** Proportion of correctly classified doublets. **C)** Proportion of correctly classified cells. **D)** Adjusted Rand Index between each tool's sample labels and the ground-truth sample labels. **E)** Balanced accuracy of each tool. **F)** Matthew's Correlation Coefficient of each tool. **G)** Area under the receiver operating characteristic curve (AUC) of the singlet assignment probability for each tool. **H)** Proportion of usable cells returned by each tool. Usable cells were defined as cells classified by singlets with an assignment probability exceeding the recommended threshold of the respective tool. **I)** Error rate amongst the usable cells returned by each tool; erroneous classifications comprised of true doublets labeled as singlets or true singlets assigned to the wrong sample.

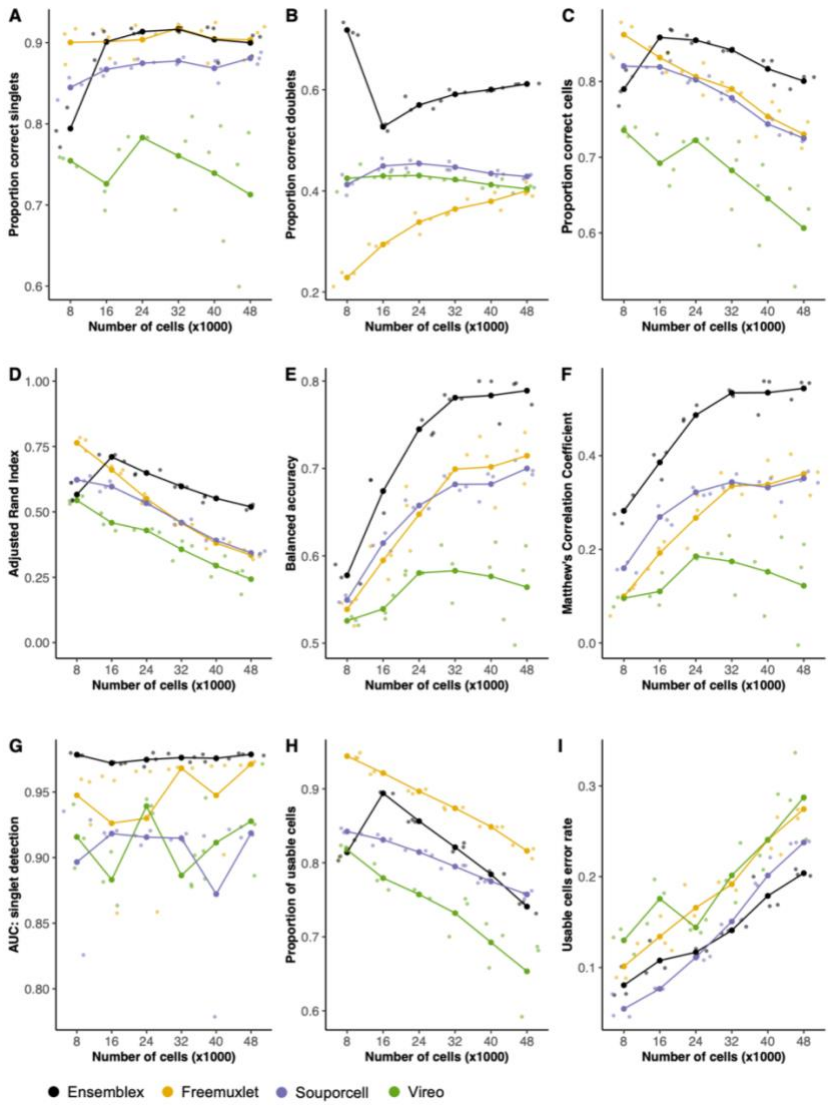

Figure S10. Genetic demultiplexing performance without prior genotype information on *in silico* pools with varying numbers of pooled cells. Genetic demultiplexing tools were evaluated on 18 *in silico* pools with known ground-truth sample labels ranging in size from 8,000 to 48,000 pooled cells with 24 multiplexed induced pluripotent stem cell (iPSC) lines from genetically distinct individuals and a doublet rate of 6% per 8,000 cells. A singlet was considered correctly classified if the assigned sample label matched the ground-truth sample label and the assignment probability exceeded the recommended threshold for the respective tool; a doublet was considered correctly classified if the assigned sample label matched the ground-truth sample label, regardless of the assignment probability. **A-I)** Line graphs showing the performance of Ensemblex and the individual genetic demultiplexing tools across evaluation metrics. The large dots show the mean value for each tool across replicates at a given pool size (n = 3 per pool size). **A)** Proportion of correctly classified singlets. **B)** Proportion of correctly classified doublets. **C)** Proportion of correctly classified cells. **D)** Adjusted Rand Index between each tool's sample labels and the ground- truth sample labels. **E)** Balanced accuracy of each tool. **F)** Matthew's Correlation Coefficient of each tool. **G)** Area under the receiver operating characteristic curve (AUC) of the singlet assignment probability for each tool. **H)** Proportion of usable cells returned by each tool. Usable cells were defined as singlets with an assignment probability exceeding the recommended threshold of the respective tool. **I)** Error rate amongst the usable cells returned by each tool; erroneous classifications comprised of true doublets labeled as singlets or true singlets assigned to the wrong sample.

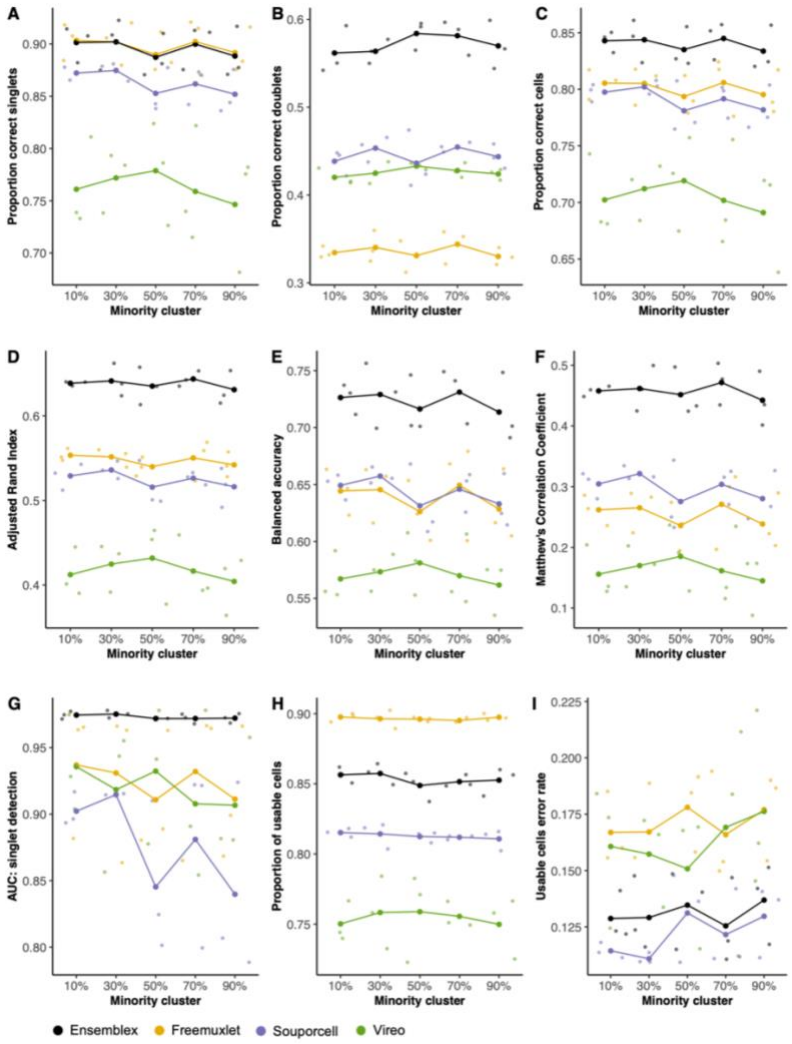

Figure S11. Genetic demultiplexing performance without prior genotype information on *in silico* pools with an underrepresented cell line. Genetic demultiplexing tools were evaluated on 15 *in silico* pools with known ground-truth sample labels, comprising 24 multiplexed induced pluripotent stem cell (iPSC) lines from genetically distinct individuals and a 15% doublet rate. For each pool, 23 iPSC lines contained 1,000 cells, while one randomly selected line showed various degrees of underrepresentation, namely 100 cells (10%), 300 cells (30%), 500 cells (50%), 700 cells (70%), or 900 cells (90%). A singlet was considered correctly classified if the assigned sample label matched the ground-truth sample label and the assignment probability exceeded the recommended threshold for the respective tool; a doublet was considered correctly classified if the assigned sample label matched the ground-truth sample label, regardless of the assignment probability. **A-I)** Line graphs showing the performance of Ensemblex and the individual genetic demultiplexing tools across evaluation metrics. The large dots show the mean value for each tool across replicates at a given degree of underrepresentation (n = 3 degree of underrepresentation). **A)** Proportion of correctly classified singlets. **B)** Proportion of correctly classified doublets. **C)** Proportion of correctly classified cells. **D)** Adjusted Rand Index between each tool's sample labels and the ground-truth sample labels. **E)** Balanced accuracy of each tool. **F)** Matthew's Correlation Coefficient of each tool. **G)** Area under the receiver operating characteristic curve (AUC) of the singlet assignment probability for each tool. **H)** Proportion of usable cells returned by each tool. Usable cells were defined as singlets with an assignment probability exceeding the recommended threshold of the respective tool. **I)** Error rate amongst the usable cells returned by each tool; erroneous classifications comprised of true doublets labeled as singlets or true singlets assigned to the wrong sample.

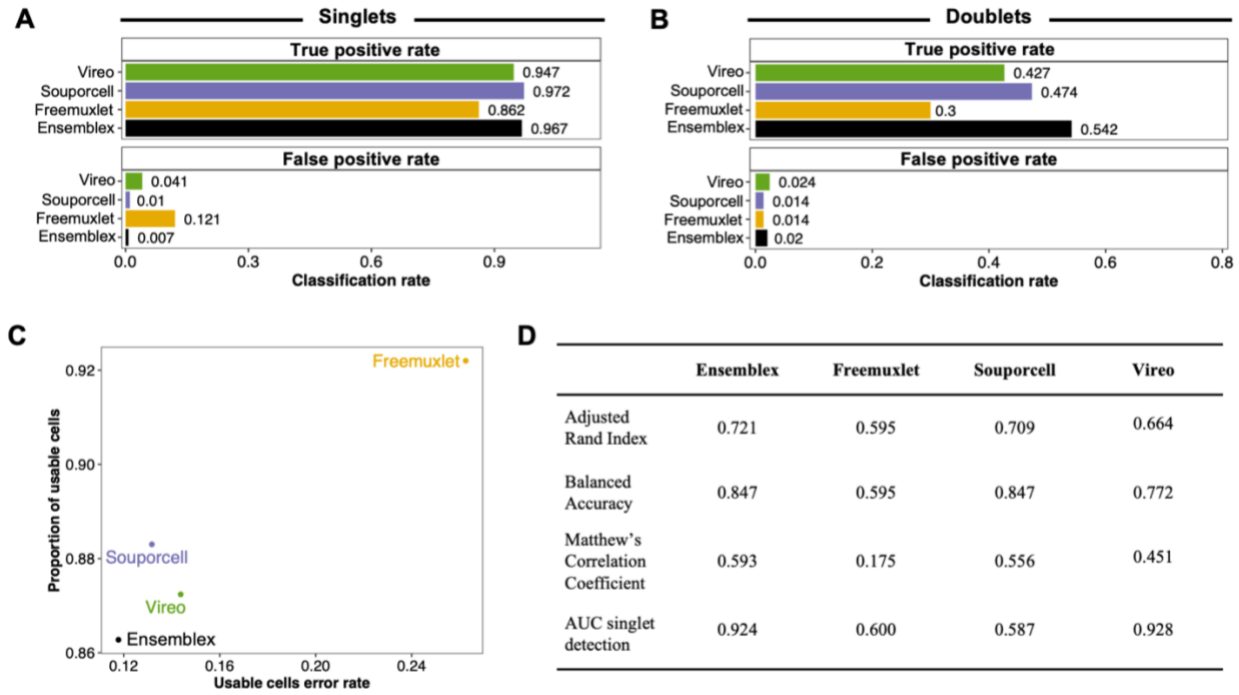

	Ensemblex	Freemuxlet	Souporcell	Vireo
Adjusted Rand Index	0.721	0.595	0.709	0.664
Balanced Accuracy	0.847	0.595	0.847	0.772
Matthew's Correlation Coefficient	0.593	0.175	0.556	0.451
AUC singlet detection	0.924	0.600	0.587	0.928

Figure S12. Evaluating Ensemblex without prior genotype information on experimentally multiplexed cells using donor-specific oligonucleotide labels as a proxy for ground-truth. Non-small cell lung cancer (NSCLC) dissociated tumor cells from seven individuals were pooled and labelled with donor-specific oligonucleotide-labels. Cells were demultiplexed according to their expression of donor-specific oligonucleotide labels by HTOdemux; HTOdemux's sample labels were used as a proxy for ground truth. True positives (TP) singlets were defined as cells classified as singlets by both HTOdemux and Ensemblex with matching sample labels; false positives (FP) singlets were defined as cells classified as singlets by both HTOdemux and Ensemblex but assigned to different donors. TP doublets were defined as cells classified as doublets by both HTOdemux and Ensemblex; FP doublets were defined as cells classified as singlets by HTOdemux and doublets by Ensemblex; false negatives (FN) doublets were defined as cells classified as doublets by HTOdemux and singlets by Ensemblex. **A)** T-distributed Stochastic Neighbor Embedding (t-SNE) visualization of HTOdemux's sample labels. **B)** T-SNE visualization of Ensemblex's demultiplexing performance using HTOdemux's sample labels as ground truth for singlets (left) and doublets (right). **C)** Bar plots showing the singlet TP and FP rates for each genetic demultiplexing tool using HTOdemux's sample labels as ground truth. **D)** Bar plots showing the doublet TP and FP rates for each genetic demultiplexing tool using HTOdemux's sample labels as ground truth. **E)** Scatter plot showing the proportion of usable cells (confidently classified singlets) and the corresponding usable cell error rate for each genetic demultiplexing tool. **F)** Adjusted Rand Index, balanced accuracy, Matthew's Correlation Coefficient, and area under the receiver operating characteristic curve (AUC) of the singlet assignment probability for each genetic demultiplexing tool.

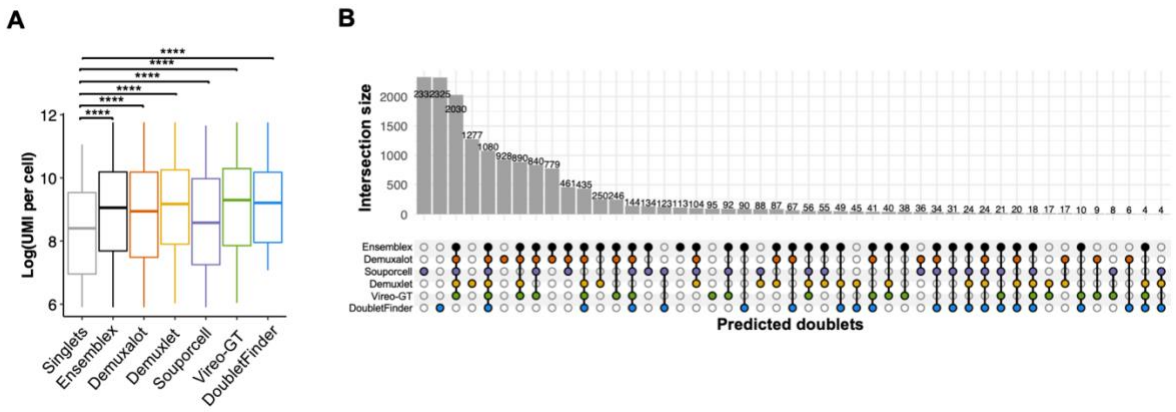

Figure S13. Doublets identified by individual tools across the dopaminergic neuron dataset. A) Boxplot showing the **distribution** of unique molecular identifiers (UMI) per cell across doublets identified by each tool and consensus singlets — cells ubiquitously assigned as singlets by each tool. Wilcoxon-rank sum tests compared the distribution of UMI per cell across singlets to that of the doublets identified by each tool. **B)** Upset plot showing the intersection of doublets identified by each tool. **** Adjusted P-value < 0.0001.

Table S1. Evaluating the contribution of each component of the Ensemblex framework to the overall demultiplexing accuracy with prior genotype information on experimentally multiplexed cells using donor-specific oligonucleotide labels as a proxy for ground-truth.

	Ensemblex demultiplexing performance		
	After Accuracy-weighted probabilistic ensemble	After Graph-based doublet detection	After Ensemble-independent doublet detection
Singlet true positive rate	0.974	0.973	0.969
Doublet true positive rate	0.518	0.589	0.662

Evaluation of Ensemblex was based on HTOdemux's sample labels. Singlet true positive rate: proportion of singlets identified by HTOdemux that had the same sample labels as Ensemblex; doublet true positive rate: proportion of doublets identified by HTOdemux that were identified as doublets by Ensemblex.

Table S2. Evaluating the contribution of each component of the Ensemblex framework to the overall demultiplexing accuracy without prior genotype information on experimentally multiplexed cells using donor-specific oligonucleotide labels as a proxy for ground-truth.

	Ensemblex demultiplexing performance		
	After Accuracy-weighted probabilistic ensemble	After Graph-based doublet detection	After Ensemble-independent doublet detection
Singlet true positive rate	0.972	0.971	0.967
Doublet true positive rate	0.417	0.485	0.542

Evaluation of Ensemblex was based on HTOdemux's sample labels. Singlet true positive rate: proportion of singlets identified by HTOdemux that had the same sample labels as Ensemblex; doublet true positive rate: proportion of doublets identified by HTOdemux that were identified as doublets by Ensemblex.

Table S3. Description of technical replicates from the dopaminergic neuron dataset.

Sequencing timepoint	Technical replicate	*n* multiplexed samples	*n* cells	ENA accession IDs
Day 11	1	22	9,314	ERR4700135 ERR4700136 ERR4700137 ERR4700138
Day 11	2	22	8,291	ERR4700139 ERR4700140 ERR4700141 ERR4700142
Day 11	3	22	10,171	ERR4700143 ERR4700144 ERR4700145 ERR4700146
Day 30	1	22	10,297	ERR4700183 ERR4700184 ERR4700185 ERR4700186
Day 30	2	22	9,486	ERR4700187 ERR4700188 ERR4700189 ERR4700190
Day 30	3	22	10,590	ERR4700191 ERR4700192 ERR4700193 ERR4700194
Day 52	1	22	8,712	ERR4700199 ERR4700200 ERR4700201 ERR4700202
Day 52	2	22	8,645	ERR4700203 ERR4700204 ERR4700205 ERR4700206
Day 52	3	22	9,240	ERR4700211 ERR4700212 ERR4700213 ERR4700214

Pooled cultures of induced pluripotent stem cell (iPSC) lines from 22 healthy donors were differentiated towards a dopaminergic neuron (DaN) fate and sequenced on days 11, 30, and 52 of differentiation by Jerber et al. For the analysis we used three technical replicates for each sequencing timepoint. ENA: European Nucleotide Archive.

Table S4. Demographic and clinical information for the subjects analyzed in the neural stem cell dataset.

Cell line	Clones	Cell type of origin	Diagnosis	Age	Biological sex
K001	i6 & i9	Keratinocytes	Healthy control	15	Male
K005	z12 & z13	Keratinocytes	Healthy control	16	Male
K011	c6 & c10	Keratinocytes	Healthy control	16	Male
K013	c20 & c20	PBMCs	Healthy control	9	Female
K015	c1 & c9	PBMCs	Healthy control	13	Male
205	c2	Lymphoblastoids	ADHD	16	Male
MR001	x3 & x15	Keratinocytes	ADHD	15	Male
MR010	c3 & c18	Keratinocytes	ADHD	9	Male
MR012	c11	PBMCs	ADHD		Male
MR013	c3 & c13	PBMCs	ADHD	16	Male
MR014	c12 & c27	PBMCs	ADHD	13	Male
MR030	c1 & c2	PBMCs	ADHD	9	Female
NR002	c2 & c21	PBMCs	ADHD	13	Male
308	c1	Lymphoblastoids	ADHD	15	Female

Table S5. Neural stem cell samples submitted for single-cell RNA sequencing and the cell lines composing their respective pools.

Experiment	Cell type	Pool	Cell line
1	NSCs	1.1	K015 c1
			K011 c10
			K013 c20
			NR002 c21
			MR010 c3
			MR014 c27
			MR030 c1
		1.2	K001 i6
			K005 z12
			K008 i13
			MR023 c17
			MR013 c13
			MR001 x3
2	NSCs	2.1	NR002 c2
			K013 c39
			MR014 c12
			K011 c6
			K015 c9
			K008 i44
			205 c2
			308 c1
		2.2	MR012 c11
			MR010 c18
			MR001 x15
			MR030 c2
			MR023 c22
			K001 i9
			K005 z13
			MR013 c3

Table S6. Distribution of putative cell types across individuals with ADHD and controls from the neural stem cell dataset according to assignments by the genetic demultiplexing tools.

	Ensemblex		**Demuxalot**		**Demuxlet**		**Souporcell**		**Vireo-GT**	
	ADHD	Ctrl	ADHD	Ctrl	ADHD	Ctrl	ADHD	Ctrl	ADHD	Ctrl
Glia	274	2355	265	2304	249	2049	514	3266	339	2521
NSC-SOX2	579	4798	590	4812	582	4120	864	4571	678	4497
NPC-POU5F1	313	3874	279	3253	295	3035	595	5574	283	2498
Neuron-DCX	680	3755	630	3740	657	3259	937	3274	745	3039
Neuron-GRIA1	413	1974	328	1647	349	1657	621	1654	207	675
NPC-S100B	385	2122	378	2117	370	1964	563	2027	447	1748
NPC-MEF2C	65	693	63	662	66	626	161	1022	84	661
NSC-APOA1	30	309	25	322	32	263	46	309	35	316